$Th_4(PO_4)_4P_2O_7$, an Original Ultralow Expansion Material

S. Launay, G. Wallez,* and M. Quarton

Laboratoire de Cristallochimie du Solide, Université Pierre et Marie Curie Paris VI, 4 place Jussieu, 75252 Paris Cedex 05, France

Received January 2, 2001. Revised Manuscript Received June 19, 2001

The thermal expansion of the thorium phosphate diphosphate has been studied from 20 to 800 °C by dilatometry and high-temperature X-ray diffraction. Both experiments indicated an ultralow expansion, with a mean global coefficient of 1.9×10^{-6} °C^{-1} over the considered range, but the phenomenon appeared to be highly anisotropic. A comparison with the known families of low- or negative-expansion compounds allowed us to conclude that $Th_4(PO_4)_4P_2O_7$ did not belong to any one of them. The Rietveld refinements of the high-temperature XRD patterns revealed no structural change but slight atomic displacements; the quasicompact packing following the *c* axis yields a normal expansion in this direction, but the distortion of the structural units leads to a very slight contraction of parameter *b* up to 300 °C, while their expansion following the *a* axis is almost damped by the tunnels of the oxygen framework. This somewhat complex structural mechanism appears to be generated by the thorium−thorium Coulombic repulsions.

Introduction

The wide field of the phosphate chemistry offers some examples of low- or negative-expansion materials, mainly because of the transverse vibration of the bridging oxygen atom in the P_2O_7 bitetrahedron of $A^{IV}P_2O_7$ compounds (A = Th, U, Hf, or Zr),[1−4] but it is also conceivable that the very rigid PO_4 tetrahedron itself plays the same role as the AlO_4 and SiO_4 tetrahedron in aluminosilicates, that is, inhibiting the thermal expansion thanks to the edges shared with larger polyhedra.[5] In some cases, like $(Zr_2O)(PO_4)_2$[6] and (U_2O)-$(PO_4)_2$,[7] low or negative expansions have been measured, but no structural explanation has been given of their thermal behavior. The present study is dedicated to a related compound: $Th_4(PO_4)_4P_2O_7$. After having long been considered as a true monophosphate,[8] a recent single-crystal XRD study has allowed the determination of its structure and correct formula.[9] It crystallizes in the orthorhombic system, space group *Pcam*, $Z = 2$, with the cell parameters $a = 12.8646(9)$ Å, $b = 10.4374(8)$ Å, $c = 7.0676(5)$ Å. It is convenient to describe this structure as an array of corner- and edge-sharing PO_4 tetrahedra and ThO_8 polyhedra forming infinite blocks extending in the (*a*,*c*) planes and stacked following the *b*-axis (Figure 1). The cross-section of the dense parts

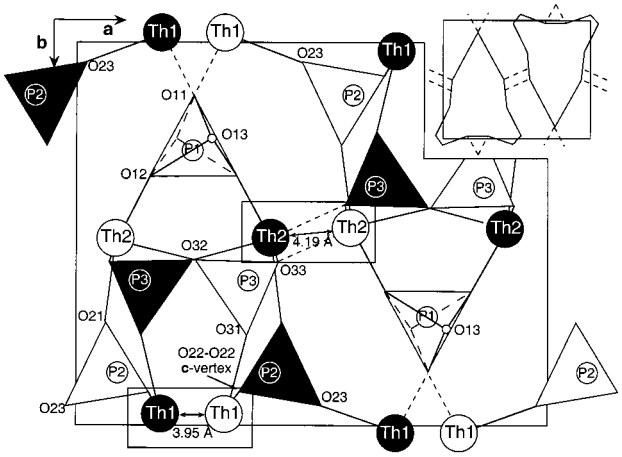

Figure 1. [001] projection of the $Th_4(PO_4)_4P_2O_7$ structure at room temperature. The atoms at $z = 1/4$ have been drawn in white, those at level $-1/4$ are in black, P(1) atoms are at $z = 0$ and 1/2. Dashed lines represent the weak "interblock" Th−O bonds. Right upper corner: the same cell, featuring the bell-shaped blocks. The oxygen environments of the thorium atoms in the rectangles are shown in Figure 2.

of the framework at $z = 1/4$ and $-1/4$ appears as *a*-directed chains made up of head-to-foot bell-shaped units (right upper corner of Figure 1) connected via the short Th(1)−O(23) bonds (2.20 Å). These chains are linked together by weak Th−O bonds (2.53−2.59 Å, dashed line; see also Figure 2) that involve less than 20% of the total valence of both thorium cations.[10] The independent $P(2)O_4$ and $P(3)O_4$ tetrahedra are almost regular. The $P(1)_2O_7$ diphosphate groups form rows extending following the *c*-axis. A position disorder led to the description of the tetrahedra as triangular bipyramids with half-occupied opposite vertexes (O13 atom). So, the "P_2O_7" group present in the formula

(1) Craig, D. F.; Hummel, F. A. *J. Am. Ceram. Soc.* **1972**, *55*, 532.
(2) Buchanan, R. C.; Walter, G. W. *J. Electrochem. Soc.* **1983**, *130*, 1905.
(3) Taylor, D. *Br. Ceram. Trans. J.* **1984**, *83*, 129.
(4) Korthuis, V.; Khosrovani, N.; Sleight, A. W. *Chem. Mater.* **1995**, *7*, 412.
(5) Sleight, A. W. *Endeavor* **1995**, *19*, 412.
(6) Yamai, I.; Oota, T. *J. Am. Ceram. Soc.* **1985**, *68*, 273.
(7) Kirchner, H. P.; Merz, K. M.; Brown, W. R. *J. Am. Ceram. Soc.* **1963**, *46*, 137.
(8) Bamberger, C. E.; Haire, R. G.; Begun, G. M.; Hellwege, H. E. *J. Less Common Met.* **1984**, *102*, 179.
(9) Bénard, P.; Brandel, V.; Dacheux, N.; Jaulmes, S.; Launay, S.; Lindecker, C.; Genet, M.; Louër, D.; Quarton, M. *Chem. Mater.* **1996**, *8*, 181.
(10) Brese, N. E.; O'Keeffe, M. *Acta Crystallogr.* **1991**, *B47*, 192.

10.1021/cm010002y CCC: $20.00 © 2001 American Chemical Society
Published on Web 09/17/2001

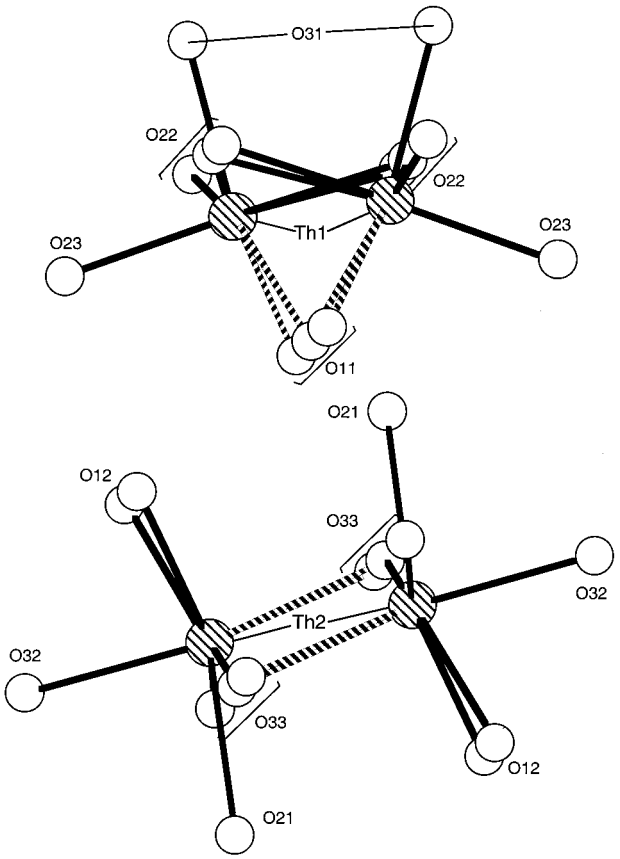

Figure 2. [001] projections with a 4° tilt of the Th(1) (above) and Th(2) (below) oxygen environments showing cross sections of the zigzag thorium chains. "Interblock" Th−O bonds are dashed lines.

appears as a *c*-oriented $-O(13)_{1/2}-P(1)O_3-$ infinite chain.

Between the bell-shaped blocks formed by the strong Th−O bonds are wide empty regions forming *c*-directed zigzag tunnels.

Experimental Procedures

Dilatometry. Thermal expansion measurements were performed from room temperature to 1000 °C, using a Unitherm Standard 1164 dilatometer (Auter Laboratory), calibrated with a silica glass standard. The samples were prepared as rectangular bars ($3.0 \times 0.5 \times 0.5$ cm^3) sintered for 12 h at 1250 °C in air; the obtained compactness was 97%.

High-Temperature X-ray Diffraction. All measurements were performed on a 17 cm vertical Philips PW1050/25 goniometer, using Ni-filtered Cu Kα radiation. A first series of X-ray patterns was recorded on a mixture of the title compound with α-Al_2O_3 as internal standard. The cell parameters of the latter were calculated at each temperature from polynomial expansion functions in order to determine the $\delta\theta = f(\theta)$ correction function to be applied to all the Bragg angles.[11] However, the cell parameter refinements resulted in rough thermal variations curves, probably because the error of the $\delta\theta$ correction was of the same magnitude as the low variations of the cell parameters. Therefore, we chose to record a second series of five patterns (from 20 to 800 °C) on pure $Th_4(PO_4)_4P_2O_7$ and to refine the instrument shift simultaneously with the crystal parameters. A total of 368 independent reflections were measured over the $8° < 2\theta < 84°$ range.

Rietveld Refinements. The Fullprof program[12] was run to refine the crystallographic and instrumental parameters, using the single-crystal data as starting values.[9] The refined data set included three cell parameters, the zero shift, the Gaussian−Lorentzian shape factor, three coefficients of the fwhm Cagliotti's polynomial, two asymmetry parameters, the overall scale factor, and 29 atomic coordinates. The isotropic displacement parameters being numerous, and for some of them of lesser importance, we decided to define a common B_{iso} variable for all the oxygen atoms but the O(13) bridging one and another variable for the P(2) and P(3) phosphorus atoms that occupy similar sites, giving a six variable set. As the grains tend to be elongated following [001] (*c* is the shortest cell parameter) and lay horizontally on the sample holder, a slight orientation anisotropy factor also had to be refined in order to correct the intensities. This factor remained almost unchanged over the temperature range. Soft distance constraints were applied on all the P−O bonds, except on the atypical P(1)−O(13) one that was left "free" in order to follow the movement of the bridging anion.

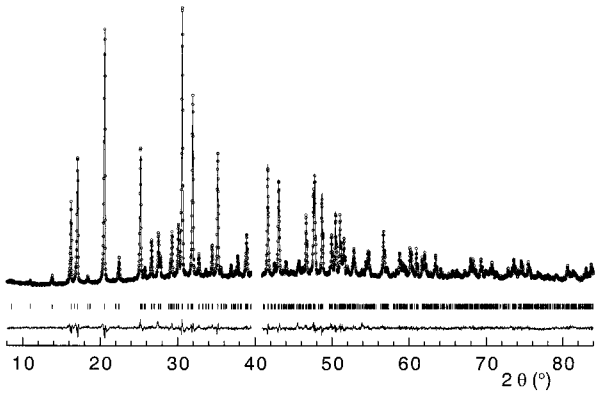

Figure 3. X-ray powder pattern of $Th_4(PO_4)_4P_2O_7$ at 800 °C: observed (circles), calculated (solid, upper plot), difference (solid, lower plot), and angular positions of Bragg reflections (bars); the excluded region corresponds to the main reflection of the platinum holder.

The refinements (Figure 3) led to fairly good reliability factors:

$$0.033 < R_P = \sum|y_o^i - y_c^i|/\sum y_o^i < 0.038$$

$$0.042 < R_{WP}\ (\text{id., weighted}) < 0.050$$

$$0.051 < R_{Bragg} = \sum|I_o^i - I_c^i|/\sum I_o^i < 0.069$$

$$0.051 < R_F = \sum|(I_o^i)^{1/2} - (I_c^i)^{1/2}|/\sum(\Sigma I_o^i)^{1/2} < 0.100$$

Results

According to the diffraction patterns, the thermal expansion of the compound appears as a very anisotropic phenomenon (Figure 4):

(1) the parameter *a* shows a near-zero expansion up to 200 °C and then increases slightly ($0 < \alpha_a < 3.0 \times 10^{-6}$ °C^{-1} between 20 and 800 °C);

(2) the expansion following the *b*-axis is still lower, with a slight contraction domain up to about 300 °C ($-0.8 \times 10^{-6} < \alpha_b < 1.5 \times 10^{-6}$ °C^{-1} between 20 and 800 °C);

(3) the parameter *c* evolves linearly over the studied temperature range, with $\alpha_c = 3.8 \times 10^{-6}$ °C^{-1}. Although the strongest of all three, this coefficient is only just half the mean one of α-Al_2O_3.[11]

(11) Taylor, D. *Br. Ceram. Trans. J.* **1984**, *83*, 92.

(12) Rodriguez-Carvajal, J. *Fullprof: Rietveld, profile matching and integrated intensity refinement of X-ray and neutron data, V 3.1.c*, Laboratoire Léon Brillouin, CEA: Saclay, France, 1997.

Table 1. Th−O Distances (Å) for the ThO_8 Polyhedra at 20 °C from Single Crystal[9] and Powder (This Work) Diffraction Data

$Th(1)O_8$	single crystal	powder	% difference	$Th(2)O_8$	single crystal	powder	% difference
Th(1)−O(23)	2.20(2)	2.33(2)	5.9	Th(2)−O(32)	2.24(2)	2.27(2)	1.3
Th(1)−O31)	2.24(2)	2.22(2)	0.9	Th(2)−O(21)	2.33(2)	2.35(2)	0.9
Th(1)−O(22)	2.44(1)	2.45(2)	0.9	Th(2)−O(12)	2.37(1)	2.41(2)	1.7
Th(1)−O(22)	2.44(1)	2.45(2)	0.4	Th(2)−O(12)	2.37(1)	2.41(2)	1.7
Th(1)−O(22)	2.52(1)	2.53(2)	0.4	Th(2)−O(33)	2.45(1)	2.44(1)	0.4
Th(1)−O(22)	2.52(1)	2.53(2)	0.4	Th(2)−O(33)	2.45(1)	2.44(1)	0.4
Th(1)−O(11)	2.59(1)	2.65(1)	2.3	Th(2)−O(33)	2.53(1)	2.58(2)	2.0
Th(1)−O(11)	2.59(1)	2.65(1)	2.3	Th(2)−O(33)	2.53(1)	2.58(2)	2.0
	$\sum s_i = 4.10^a$	$\sum s_i = 3.73^a$			$\sum s_i = 4.30^a$	$\sum s_i = 4.02^a$	

[a] Cumulated valences calculated from ref 10.

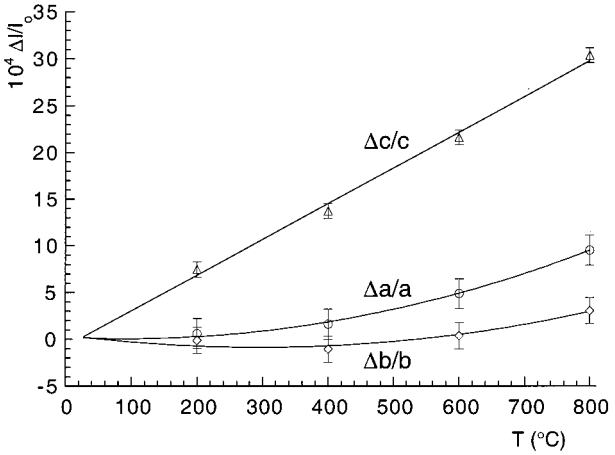

Figure 4. Thermal expansion of $Th_4(PO_4)_4P_2O_7$ following the *a*, *b*, and *c* axes.

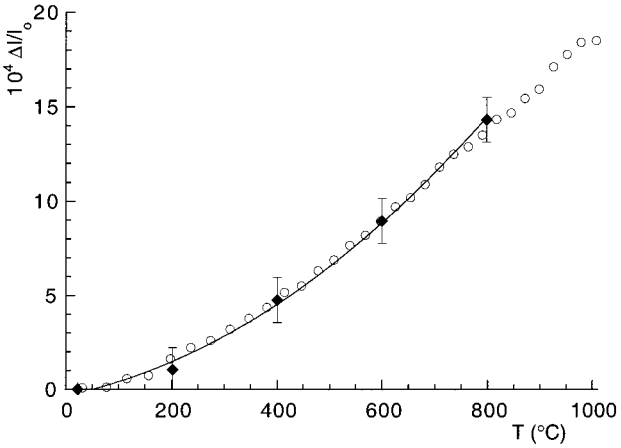

Figure 5. Relative thermal expansion of a sintered bar (circles) and calculated from the HTXRD-refined cell parameters (black squares).

As shown by Figure 5, the mean thermal expansion ($\Delta l/l = (\Delta a/a + \Delta b/b + \Delta c/c)/3$) is consistent with the dilatometric measurement; this means that the macroscopic phenomenon results only from the thermal evolutions of the crystal structure, not from a sintering shrinkage. The regression parabola calculated from the dilatometric data shows that the linear expansion coefficient ($\alpha_g = (\alpha_a + \alpha_b + \alpha_c)/3$) increases from 1.1 × 10^{-6} °C^{-1} at 20 °C to 2.9 × 10^{-6} °C^{-1} at 1000 °C, with a mean value of 1.9 × 10^{-6} °C^{-1}. According to the common classification of thermal ceramics[13] [very low expansion ($\alpha_b < 2 \times 10^{-6}$ °C^{-1}), low expansion ($2 \times 10^{-6} < \alpha_b < 8 \times 10^{-6}$ °C^{-1}), and high expansion ($\alpha_b > 8 \times 10^{-6}$ °C^{-1})], $Th_4(PO_4)_4P_2O_7$ appears as a very low expansion material.

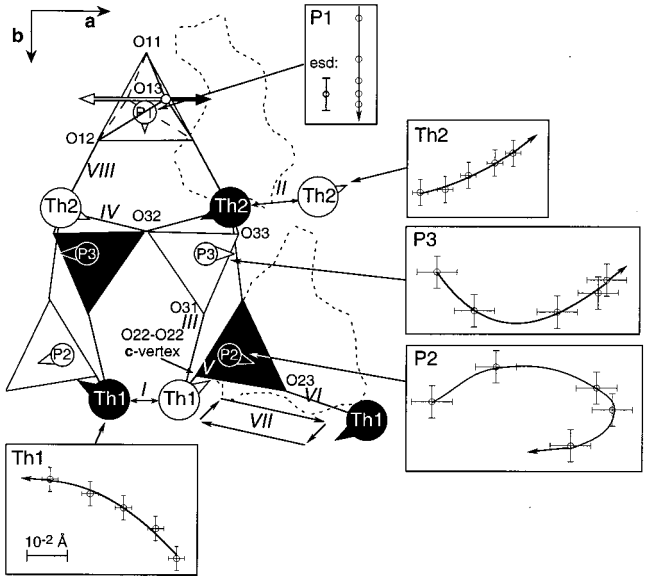

Figure 6. [001] projection showing the thermal evolution of the structure. The movement of each kind of cation (positions and esds at 20, 200, 400, 600, and 800 °C at heating; 100× magnified) is shown beside. The dashed lines show the cross sections of the cavities at $z = 1/4$.

From a structural point of view, one can compare the Rietveld-refined structure at 20 °C with that determined from single-crystal diffracted intensities.[9] Both are very similar, while differences up to 6% are found between homologous Th−O bond lengths (Table 1), probably because of unfavorable experimental conditions such as the presence of heavy atoms, the different limits of the scan ranges, or the well-known lack of reproductibility between single-crystal and powder data. However, we will ignore these systematic differences and focus on the thermal variations themselves, which are significantly stronger than the esds (Figure 6).

Discussion

In a recent survey of materials that contract on heating, Sleight reported the known structural mechanisms that lead to negative thermal expansion along one or more directions.[14] In the following discussion, we will take up his classification in order to try to place the present compound among the different families.

(13) Roy, R.; Agrawal, D. K.; McKinstry, H. A. *Annu. Rev. Mater. Sci.* **1989**, *19*, 59.

(14) Sleight, A. W. *Inorg. Chem.* **1998**, *37*, 2854.

First, one can consider a material with a cation showing a very distorted coordination polyhedron at low temperature that becomes more symmetric on heating. By getting more regular, the polyhedron reduces in size, resulting in a contraction along one axis, as in the tetragonal ferroelectric form of $PbTiO_3$. In $Th_4(PO_4)_4P_2O_7$, at room temperature, the thorium atoms are clearly off-centered, with distances to the barycenter of their neighbor oxygen anions of 0.32 Å for Th(1) and 0.20 Å for Th(2), but instead of fading on heating, these values follow a slight increase to respectively 0.37 and 0.22 Å at 800 °C. Furthermore, there is almost no change in the shape of the coordination polyhedra over the investigated temperature range. The opposite behaviors find their explanation in the structural differences between $Th_4(PO_4)_4P_2O_7$ and the lead perovskites:

(1) in the latter ones, the symmetry increase is mostly due to the loss of the lone pair effect of the lead II $6s^2$ electrons at high temperature, a phenomenon that does not occur in the former;

(2) as shown above, the structure of the title compound is made up of *b*-stacked blocks that impose highly anisotropic thorium polyhedra (Figure 2), with strong intrablock bonds within one hemisphere and weak extrablock ones on the other side; this prevents any spherization of the thorium environment.

The second family consists of compounds with edge- or face-sharing polyhedra, one of them being made of strongly covalent bonds that prevent or limit the thermal expansion. On the contrary, $Th_4(PO_4)_4P_2O_7$ is a basically monodentate structure with few common edges, all *c*-oriented, that is, following the axis of highest thermal expansion. We can conclude that the shared edges do not play the expected role and that $Th_4(PO_4)_4P_2O_7$ does not belong either to the second family.

The compounds of the third and largest group are made up of rigid corner-sharing MO_n polyhedra. The angle of the M−O-M linkage, typically near 180° at low temperature, decreases at heating due to the transverse motions of the oxygen atom, resulting in shorter M−M distances. Because the "rocking polyhedra" phenomenon is quite common among the compounds with M_2O_7 bitetrahedral units, the present work was initially undertaken in order to clear up the role of the $-O(13)_{1/2}-P(1)O_3-$ infinite chain extending following *c* in the low expansion of $Th_4(PO_4)_4P_2O_7$. However, it soon became evident that the rocking mechanism was not the right explanation insofar as this axis, as was mentioned above, is the one of highest thermal expansion.

As shown by this brief survey, the thermal behavior of $Th_4(PO_4)_4P_2O_7$ does not obey any of the three classical models of low thermal expansion compounds, and indeed, a thorough examination of the thermal evolution of the structure was necessary to find its origin.

In the following discussion, particular attention will be paid to the movements of the cations, as they provide the most significant information concerning the structural evolution and also the most reliable ones due to their atomic weights. Some tetrahedra rotations probably occur, but they are faint and do not appear clearly from the movements of the oxygen anions. However, we shall follow with interest the displacements of the atypical O(13) bridging anion. The cations movements shown in Figure 6 are very gradual and greater than the esds on the coordinates. They have been also summarized by simple shifts over the temperature range (Table 2).

Table 2. Cations and O(13) Displacements[a] (10^{-4} Å, Esds in Parentheses) between 20 and 800 °C

	Th(1)	Th(2)	P(1)	P(2)	P(3)	O(13)
Δx	−31(3)	−24(4)	0	34(8)	−42(8)	210(120)
Δy	−19(5)	−10(6)	21(8)	−11(8)	2(8)	<esd

[a] These displacements are relative to the atomic coordinates published in ref 9.

The driving forces of this somewhat complex displacement mechanism appear clearly to be the repulsions between neighbor thorium atoms, resulting from three factors:

(1) the very electropositive character of the thorium atom ($\chi = 1.11$),[15] which induces a high real charge and strong electrostatic interactions;

(2) the surprisingly short first Th(1)−Th(1) and Th(2)−Th(2) distances at room temperature (respectively twice 3.947 and 4.192 Å), whereas the next ones are far greater (respectively twice 5.894 and 5.500 Å);

(3) the absence of screening oxygen anions between two neighbor thorium atoms.

So, as the temperature increases and the structure softens, these repulsions relax by lengthening the shortest Th(1)−Th(1) and Th(2)−Th(2) distances by about 1% over the 20−800 °C range (Figure 6, interactions I and II).

The *c*-projection shows how these displacements also affect the neighbor PO_4 tetrahedra:

(1) the shifts of both the Th(1) and Th(2) atoms induce the displacement of the coplanar $P(3)O_4$ tetrahedron by pushing along the very short Th(1)−O(31) and Th(2)−O(32) bonds, both 2.24 Å long (interactions III and IV);

(2) Th(1), bonded to two O(22) vertexes of two $P(2)O_4$ tetrahedra (images by the *m* mirror), also pushes them in a roughly parallel direction (interaction V), but the $P(2)O_4$ tetrahedron itself pushes another Th(1) atom via the short O(23)−Th(1) bond (interaction VI), leading to a circular movement as drawn at the bottom of Figure 6 (VII); this accounts for the fact that neighbor Th(1) atoms do not shift in exactly opposite directions as it is the case for the Th(2) ones;

(3) the $-O(13)_{1/2}-P(1)O_3-$ chain, extending along [001], is pulled by the short Th(2)−O(12) bonds (2.37 Å) and follows the displacement of Th(2) by shifting along the *b* axis (interaction VIII).

One should note that both Th(1), the $P(2)O_4$, and $P(3)O_4$ tetrahedra shift toward the tunnels, but not Th(2), because of the short extrabell Th(2)−Th(2) distance. Therefore, the bells flatten as temperature increases (the shrinkage following *b* can be correlated to the slight reduction (0.004 Å) of the intrabell Th(1)−P(1) distance), while the bases tend to broaden (expansion following *a*) (Figure 7). This allows us to explain the atypical thermal behavior of the material in the (*a*,*b*) plane:

(1) following *a*, the broadening of the bells has almost no effect on the cell parameter, first because it occurs toward free spaces, second because the $Th(1)-P(2)O_4-$ $Th(1)-P(2)O_4-$ circular movement allows the shearing shifts of the bells;

(15) Allred, A. L.; Rochow, E. G. *J. Inorg. Nucl. Chem.* **1958**, *5*, 264.

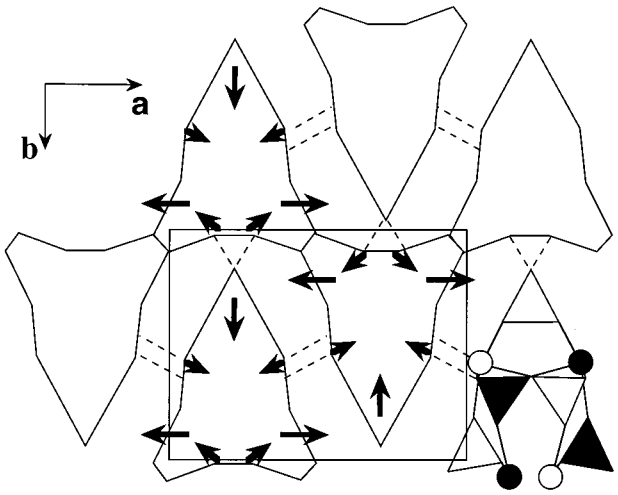

Figure 7. [001] projection showing the deformation of the "bell" structural units and the global expansion mechanism. The "interblock" Th−O bonds are dashed lines.

(2) the flattening of the bells following *b* results in a direct reduction of the associated cell parameter.

As the thorium atoms are constrained by symmetry to lie in the $z = 1/4$ and $-1/4$ mirror planes, the Th−Th electrostatic repulsions following *c* implies the increase of the corresponding cell parameter, resulting in a more usual expansion coefficient. At the same time, one can observe a strong shift of the O(13) bridging atom along *a*. Because the distance to its P(1) neighbors does not vary significantly [from 1.88(3) Å at 20 °C to 1.83(2) Å at 800 °C], we can assume that this movement [roughly toward the P(1)−P(1) axis] answers to the necessity to keep in contact with the two cations.

The incurved displacement of the P(2) and P(3) atoms can be probably attributed to a rotation of the PO_4 tetrahedra. Due to the uncertainties on the oxygen positions, we cannot determine precisely this effect, which is only a consequense of the movements of the thorium atoms.

Conclusion

$Th_4(PO_4)_4P_2O_7$ appears as an atypical compound that does not obey the heretofore known mechanisms leading to low or negative thermal expansion. Unlike in other diphosphates, the origin of the phenomenon is not to be found in the bridging oxygen atom but in the coexistence of favorable factors, that is, high-charge cations at short distances, a noncompact structure, and a monodentate oxygen framework. Such features may be found in already known compounds, and although their structures are slightly different, it is possible that a similar mechanism occurs in $(Zr_2O)(PO_4)_2$ and $(U_2O)(PO_4)_2$, for which a HTXRD study is in progress.

Acknowledgment. The authors are grateful to N. Lequeux (Laboratoire des Céramiques et Matériaux Minéraux, UPMC-Paris) for performing the dilatometry experiments and to J.-P. Souron (Laboratoire de Cristallochimie du Solide, UPMC-Paris) for the HTXRD measurements.

Supporting Information Available: X-ray refinement data for $Th_4(PO_4)_4P_2O_7$ at various temperatures. This material is available free of charge via the Internet at http/::pubs.acs.org.

CM010002Y